Hanen *et al.*
Bulletin of the National Research Centre (2023) 47:132
https://doi.org/10.1186/s42269-023-01103-z

Bulletin of the National
Research Centre

RESEARCH
Open Access

Novel composite membrane based on recycled low-density polyethylene-alumina used for vacuum membrane distillation

Ajari Hanen[1], Khaled Fatma[1], Akrout Hiba[1], Hidouri Khaoula[1*], Chaouachi Béchir[1] and Alsalhy Qusay[2]

Abstract

Background Plastic materials have a significant impact on the entire environment. Very relevant ideas in different areas with the aim of enhancing these materials and making them effective in our daily lives. In this context, our work in this article by using plastic materials in the manufacture of hydrophobic membranes realized in our Laboratory LEEP Enig Gabes Tunisia, followed by various analyses. These membranes are made of a Recycled Low-Density Polyethylene polymer by means of the Thermal Induced Phase Separation (TIPS) method by using solvents such as Butyl Acetate, non-solvent Hexane with the addition of Alumina at different concentrations to increase porosity.

Results Hydrophobic membranes are coupled to the vacuum still to test their performance. An analytical study by FTIR was done. Contact angle, pore size, porosity, mechanical test, bubble point pressure, AFM and SEM analysis. The results revealed that the addition of alumina had an important role in improving the structure, properties and therefore the performance of the membrane.

Conclusions The membrane already prepared admits according to the analyzes tested a good porosity, hydrophobicity.

Keywords Recycled low-density polyethylene, Alumina, Membrane, Hydrophobic, TIPS

Background

Since antiquity, water has had a primordial value in our land. Their importance grows more and more given the population growth. Making wastewater safe to drink is a worldwide challenge. In addition, even drinking water becomes polluted due to the enormous use, mainly of plastic materials. Faced with this serious problem, several research works are working continuously to solve these water problems. According to studies conducted by the UN, one in four people or two billion people in the world—lack of drinking water and 1.4 million people die (Hamad et al. 2013), thus, desalination becomes a necessity for this important issue (Wang and Chung 2015). What drives all of the research to focus on the filtration and desalination of water to produce large amounts of purified water in a short time with less investment. Many technologies have been produced in this context: thermal processes such as the known one, such as (MSF, MED, MED-TC), processes with the use of membranes such as reverse osmosis (RO), and the hybrid process such as membrane distillation (MD) (Chang et al 2019). The choice of one of these techniques is the basis of several processes: fresh, water suitability, impactful of the environment. Currently, DM is a widely used technology; this technique is used more nowadays (Aljumaily et al.

---

*Correspondence:
Hidouri Khaoula
khaoula2013@yahoo.fr
[1] Research Laboratory: Energy, Water, Environment and Processes, ENIG: Universite de Gabes, Ecole Nationale d´Ingenieurs de Gabes, Gabès, Tunisia
[2] Membrane Technology Research Unit, Department of Chemical Engineering, University of Technology-Iraq, Alsinaa Street 52, Baghdad 10066, Iraq

2022; Khaled et al. 2020; Asma et al. 2020), with very significant rejection yields manifests itself as a promising alternative (Asma et al. 2022) due to its advantages such as low salt rejection. For this, it is necessary to couple membrane process with renewable energies such as solar energy (Fatma et al. 2017). In this work, membrane distillation under solar vacuum was studied for water desalination. The study is based on everything on the motor organ which is the membrane in the MD processes. Several have their work on the manufacture of membranes in various materials, to prepare hydrophobic porous membranes (Aljumaily et al. 2019) such as PVDF, PTFE, PP and PE. All these studies showed promising results, but despite everything, the cost of the polymer is very high and the cost of MD membranes (Abedini et al. 2014). Therefore, in this work, recycled low-density polyethylene was used to prepare a flat sheet membrane for VMD application to increase the production of potable water and at the same time get rid of solid waste. This material is used for several reasons like being very cheap, hydrophobic in nature, low surface energy similar to PVDF and PP, good chemical stability and very low thermal conductivity (Malinalli et al. 2023; Ajari et al. 2019). Nowadays, composite membranes have gotten a lot of attention due to their flexibility of having more than one layer and using a variety of materials to form the membrane. In this article, a composite membrane was prepared using recycled low-density polyethylene (RLDPE), thus helping to lighten the burden of plastics on the environment, while alumina powder was used to reinforce these membranes and improve its properties for better MD efficiency. Several studies are based on the manufacture of PE membranes for MD using melting/cold stretching extrusion methods (El-Bourawi et al. 2006). In addition, the use of thermally induced phase separation (TIPS) methods in the preparation of PE membranes is very suitable, especially for semi-crystalline polymers that cannot be easily dissolved by solvents like LDPE (Tobo-Niño et al. 2017). In this study, flat sheet membranes were fabricated by the TIPS method and tested in solar vacuum membrane distillation (SVMD) for the desalination of seawater and brackish water.

Methods

Materials

Recycled polymers (RLDPE) were supplied from plastic manufacturing company located in Gabes (Tunisia). Butyl acetate and hexane were purchased by Laboratory Reagents & Fine. Chemicals, LOBA Chemie PVT.LTD.

Fabrication of AL/RLDPE composite membrane

In order to obtain flat membranes, the polymer solution called «collodion» is first prepared. A mixture of butyl acetate is used as a solvent in the preparation of all collodions (Fig. 1). The polymer mixture Rd is dissolved by adding the alumina powder with different amounts in the solvent under magnetic agitation in an oil bath at 130 °C until the polymer is completely dissolved. Once the collodion is prepared, it is spread on a glass plate using a manual film applicator. The resulting film is exposed to atmospheric conditions for 5 min then immersed in hexane and ethanol to extract the solvent from the membrane after it has been dried in an oven at 70 °C. Finally, the membrane is left at room temperature for 24 h before characterization analyses. Using an atomic force microscope (Brucker Nanoscope, France), the analysis topography of flat sheet membrane was assessed. After obtaining the membrane surface's 3D surface topography, the surface roughness was determined. According to the following statement (Rasool and Vankelecom 2021):

$$\mathrm{Ra} = \frac{1}{\mathrm{L}x\mathrm{L}y}\int_{0}^{\mathrm{L}y}\int_{0}^{\mathrm{L}y}\left|Z(x,y)\right|\mathrm{d}x\mathrm{d}y \tag{1}$$

where Ra is the roughness, Z (x, y) is the surface relative to the median plane, Lx, Ly are the dimensions of the area.

The sessile drop method was used to measure the membrane contact angle (CA). In order to accomplish this, a micro-syringe was employed for injecting a drop

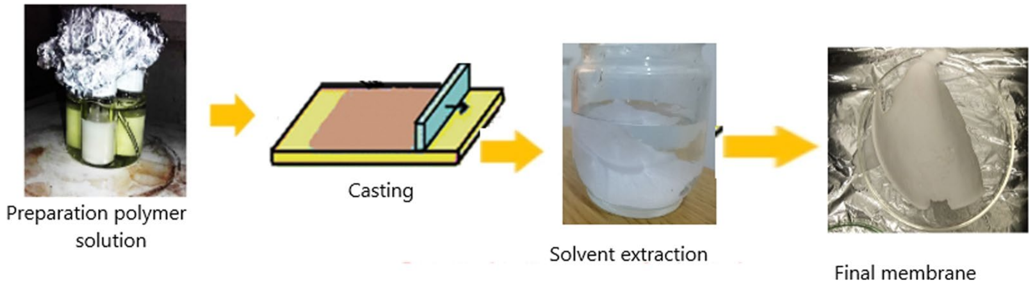

Fig. 1 Experimental setup of the preparation of flat sheet membranes

of bidistilled water onto the membrane. After that, a goniometer (CAM100 apparatus, Italy) was utilized to measure the contact angle. Six different positions on the membrane were measured, and the average value and its associated standard deviation were determined.

Membrane morphology, porosity, pore size and bubble point

The membrane morphology was investigated by evaluating SEM pictures taken with a (Zeiss EVO MA10, Switzerland) SEM. Membranes cross sections were obtained by freezing the samples in liquid nitrogen, resulting in a crisp brittle fracture. Before the SEM test, a tiny layer of gold was applied to the membrane samples to make them conductive. The overall porosity of the membrane can be calculated by the following expression (Asma et al. 2021)

$$\varepsilon\% = \frac{(w_{\mathrm{w}} - w_{\mathrm{d}})/\rho_{\mathrm{k}}}{(w_{\mathrm{w}} - w_{\mathrm{d}})/\rho_{\mathrm{k}} + w_{\mathrm{d}}/\rho_{\mathrm{p}}} * 100 \tag{2}$$

where w_{d} is the mass of the dry sample (g), w_{w} is the mass of the wet sample (g), ρ_{k} is the density of the kerosene (0.82 g/cm^3), and ρ_{p} is the density of the polyethylene (0.92 g/cm^3).

The dried membranes were cut, weighed and then, immersed in kerosene. After a few hours, the samples were taken, washed to remove kerosene stuck to the surfaces of the membranes and reweighed. The average pore size and bubble point of flat sheet membranes were measured using a wet/dry method using a pore wick (surface tension of 16 dynes/cm) as the wetting liquid and a porometer at capillary flow (CFP 1500 AEXL, Porous Materials Inc., USA). First, when the first bubble of pure nitrogen was admitted into the membrane, the nitrogen pressure was found to exceed the capillary flow of fluid inside the larger pore. The pressure was then increased until the flat sheet membrane dried, which meant that all pores were empty of the pore wick. The attached software calculated the pore size based on the nitrogen flow rates through the wet and dry membranes. Tensile proprieties. The mechanical properties of flat sheet membranes were measured with a (ZWICK/ROELL Z 2.5 test unit, ITM-CNR Italy). For each membrane, three samples (1* 5cm^2) were examined. Each one was stretched at a constant rate of 5 mm/min in unidirectional strain. The strain at break, tensile strength, Young's modulus or elastic modulus, and breaking elongation were all evaluated.

Membrane applications: VMD experiments

The VMD tests have been carried out in the laboratory device illustrated schematically in Fig. 2. The membrane was inserted between the upper (feed side) and bottom (permeate side) compartments. The effective area of the membrane was computed based on the area of the membrane exposed to the vacuum space and was 12 cm^2. The feed solution was cycled upstream of the membrane and passed through a heating water bath (Carlo Gavazzi, PDI409, Tunisia) outfitted with a temperature controller of 0.1 °C accuracy. The feed was continually churned at atmospheric pressure during the trials, and the temperature was changed between 25 and 90 °C. To extract the vapor, the permeate side was connected to a vacuum pump. The downstream pressure was between 0.2 and 0.9 bar. Permeate was condensed in a liquid nitrogen-immersed cold trap, and the collected permeate was weighed every hour to examine flux variation. The following expression can be utilized for determining the permeate partial flux Ji of the component i:

$$Ji = \frac{mi}{(A\Delta \mathrm{t})} \tag{3}$$

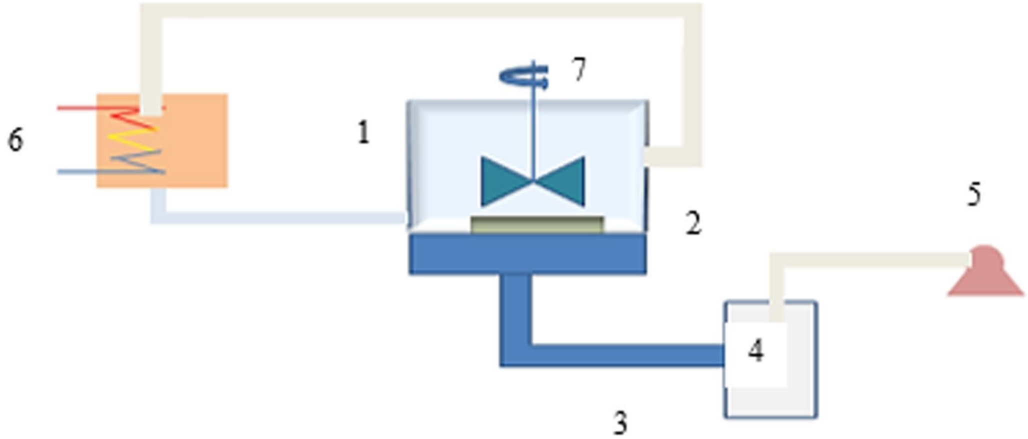

Fig. 2 Schema of the device VMD: 1. Feed reservoir; 2. Membrane; 3. Permeate; 4. Condenser; 5. Vacuum pump; 6. Temperature control with heating oil; 7. Mixer

All VMD experiments were repeated at least two times in order to check the reproducibility of the measurements.

Discussion

Membrane hydrophobicity and roughness

Measurement of the contact angle (Figure a, b) is an experimental technique used to assess the hydrophobic character of the surfaces. If the angle of contact is between 0° and 90°, the material is hydrophilic and hydrophobic, if the angle of contact is between 90° and 180°. In our work, we found a contact angle of the order of 115°, which proves that it is a hydrophobic membrane. Furthermore, the roughness and contact angle have a strong relationship. Roughness improves wettability, according to Wenzel RN 1936 (Marino et al. 2019; Ajari et al. 2019) and can be predicted with the Wenzel (1936) relation as follows:

$$\cos\theta^{*} = r\cos\theta \tag{4}$$

Wenzel defined the roughness ratio as $r = a/A$, If the factor r is larger than 1, a hydrophilic solid ($\theta < 90°$) becomes more hydrophilic.

When rough ($\theta^{*} < \theta$). Conversely, a hydrophobic solid ($\theta > 90°$) shows increased hydrophobicity ($\theta^{*} > \theta$).

As a result, the topography of the surface of the manufactured membrane was investigated using an atomic force microscope. In this example, AFM was carried out using Nanoscope III equipment (Bruker, Santa Barbara, USA).

Figure 3b shows the obtained membrane's AFM picture. The resulting membrane has the greatest roughness of 527 nm, as can be shown. The properties of an RLDPE-alumina (RLDPE-Al2O3) membrane synthesized via thermal induced phase separation (TIPS) utilizing butyl acetate as a solvent are shown in Table 1.

Table 1 Properties of the obtained membrane

Membrane		
Proprieties		**RLDPE-Al_2O_3**
Contact angle (°)		115
Roughness (nm)		527
Porosity (%)		65
Pore size (μm)		0.1097
Bubble point pressure (bar)		0.593
Mechanical properties	Mod(N/mm^2)	323.34
	Ebreak (%)	117.83
Permeate flux (Kg/m^{2}h)		1.187

Porosity, pore size and bubble point pressure

The membrane porosity is defined as the ratio of the volume occupied by pores to the total volume of the membrane. A higher porosity of a porous membrane means an increased surface area available for evaporation. The membrane porosity for MD can range from 30 to 85% (Alkhudhiri et al. 2012; Cipollina et al 2012). The obtained membrane, as indicated in Table 1, exhibits a porosity value of 65%. This suggests that the membrane possesses a favorable level of porosity, making it appropriate for utilization in membrane distillation applications.

Table 1 displays the pore size of the obtained membrane as 0.1097 μm. It is noteworthy that in membrane distillation, membranes with pore sizes ranging from 100 to 1 μm are commonly employed to prevent liquid penetration, as reported. The pore size of the obtained membrane falls within this recommended range. The pore size of a prepared RLDPE-alumina membrane plays a crucial role in determining the permeate flux. A higher pore size in the membrane corresponds to an increased permeate flux. Therefore, it is essential to identify the optimal pore size for each membrane distillation (MD) process based on the specific operating conditions. By carefully

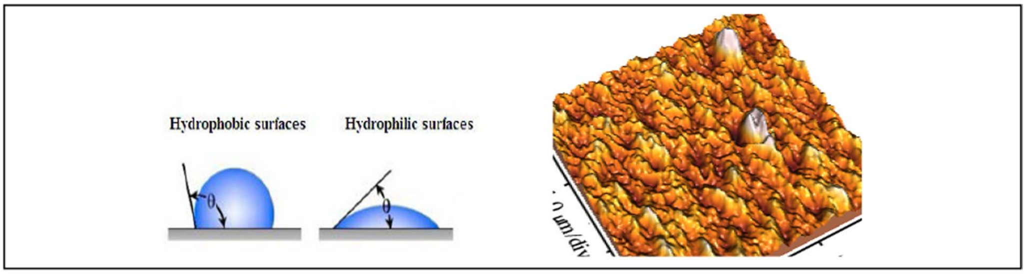

a) Contact angle of the obtained membrane, b) AFM image of the obtained membrane

Fig. 3 **a** Contact angle of the obtained membrane, **b** AFM image of the obtained membrane selecting and controlling the pore size, it is possible to enhance the efficiency and performance of the MD process.

Membrane morphology

SEM (scanning electron microscopy) was employed to analyze and characterize the morphology of the obtained membrane. This technique allows for high-resolution imaging of the membrane's surface and cross-section, providing valuable insights into its structural features and porosity. Figure 4 illustrates SEM images of the top and bottom surfaces of the obtained membrane. Additionally, Fig. 4 exhibits SEM images illustrating the cross section of the obtained membrane. The analysis of these images revealed a leafy structure with a random orientation, highlighting the porous nature of the membrane. Moreover, distinct stratified lamellae was observed, which can be attributed to the high degree of crystallinity in the LDPE polymer. Indeed, these observations are consistent with the findings of Douglas R. Lloyd's study in 1990 which highlighted that semi-crystalline and crystalline polymers have the ability to form intricate folded chains and supra-molecular architectures, such as axialites and spherulites. The presence of well-defined stratified lamellae in the cross section of the obtained membrane further supports the notion that the LDPE polymer used in the membrane exhibits semi-crystalline characteristics, confirming the resemblance to axialites and spherulites, as proposed in Lloyd's study. This observed morphology can be attributed to the solid–liquid demixing process that takes place during the cooling of the film. As mentioned by Ji et al. (2008), when membranes are fabricated using the TIPS (Thermally Induced Phase Separation) method, a significant portion of the solvents present in the film is expelled from the spherulites (matrix polymer) during the process of polymer crystallization. This expulsion occurs if the temperature reaches the crystallization temperature of the polymer.

Mechanical proprieties

The material stress–strain behavior can be determined by analyzing the recorded forces and displacements, taking

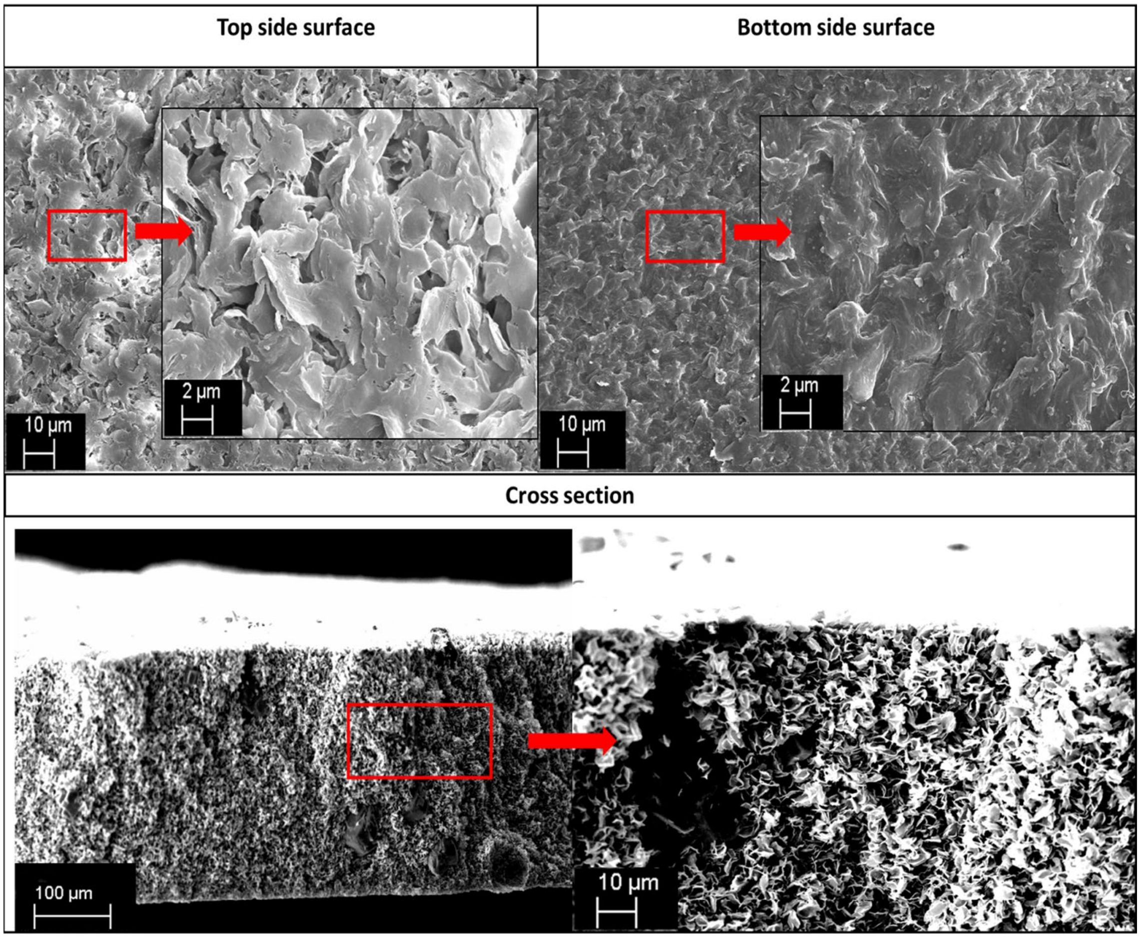

Fig. 4 SEM image of the surface (top and bottom side) of the obtained membrane

into account the sample's cross-sectional area and loading mode, as indicated by Vinci and Vlassak (1996). In this study, three samples with a cross-sectional area of 1*5 cm^2 were tested for each membrane. The mechanical properties of the obtained flat sheet membrane were evaluated by subjecting each sample to unidirectional strain at a constant rate of 5 mm/min. The results, including tensile strength, strain at break, elastic or Young's modulus, and breaking elongation, are presented in Table 1.

Notably, the obtained membrane exhibited a high strain at break, reaching 117%. This indicates that the membrane possesses significant elasticity. The presence of a lamellae structure, formed through the Liquid–Liquid phase separation process, may be a contributing factor to its high elasticity.

The strain-induced microstructural changes in membranes can be substantial, which challenges several assumptions typically made about plastic deformation in bulk materials, such as in-plane elastic isotropy, as highlighted by Kui et al. (2017). Therefore, it is crucial to accurately analyze the mechanical properties of membranes while considering the underlying mechanisms. This approach is necessary for optimizing membrane design and processing to ensure long service life. A comprehensive analysis of the mechanical properties of membranes, coupled with a thorough understanding of the underlying mechanisms, is vital for the effective design and processing of membranes to achieve long-lasting performance (Kui et al. 2017).

Effects of feed temperature and transmembrane pressure

The effect of the feed pressure on the permeate flux for the different temperatures is given in Fig. 5. The test is carried out with seawater with a salinity of 8 g/l. It is also noted that the permeate flux increases linearly with the supply temperature of the hot fluid; this result is consistent with the research of Yongqing W et al. in 2015. This observed increase is due to the increase in the driving force of the transfer (the transmembrane vapor pressure gradient). Plus, the effect of vacuum pressure on system performance. As shown in this figure, the permeate flow goes from 0.2 to 0.6 l/h.m2 when the vacuum varies from 0.2 bar to 0.7 bar. This is because the flux of water permeate gradually decreases with increasing pressure due to the loss of the driving force across the membrane. The greater the difference between the membrane pressure on the permeate side and the water-saturated vapor pressure at the system temperature, the greater the driving force of the DMV process. To create the vacuum, the energy represents only 2% of the total energy. This finding is consistent with research conducted by Abdallah H in 2014. Comparison of different membranes used in VMD. Table 2 presents a comparison of the permeate flux values achieved by different membranes used in Vacuum Membrane Distillation (VMD) for water desalination, as reported in the literature, alongside the permeate flux obtained in the current study. Upon comparing the permeate flux values from this study with those from other studies, it is evident that they are quite similar. This is an encouraging result, particularly considering that the starting polymer used in this study is recycled. The similarity in permeate flux between the current study and previous research indicates that the performance of the membrane developed in this study is comparable to membranes fabricated using virgin polymers.

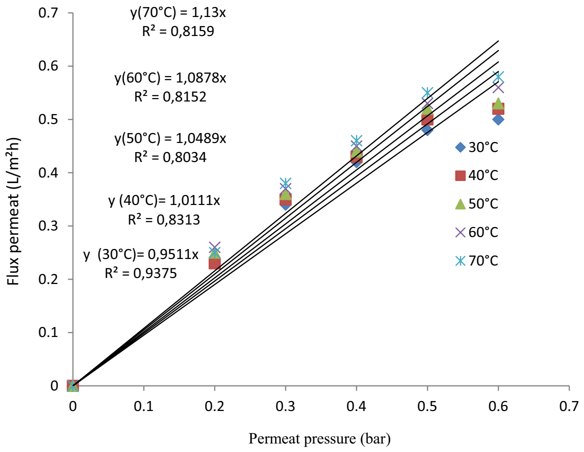

Fig. 5 Effect of the feed temperature and the transmembrane pressure on the permeate flux

Conclusions

In this work, a novel composite flat sheet membrane was prepared, characterized, and utilized in vacuum membrane distillation for desalinating seawater and brackish water. The flat sheet membrane was prepared using a recycled polymer, specifically low-density polyethylene

Table 2 Comparison of the VMD performance of different membranes found in the literature with the current RLDPE-Al2O3 membrane

Membrane	Feed temperature (°C)	Vacuum pressure (bar)	Permeate flux (kg/m^2h)	References
PVDF	27	0.0378	0.692	[31]
Polypropylene	60	0.59	0.25	[29]
ANN model	60	0.59	0.43	[32]
RLDPE-Alumina	60	0.6	0.432	This study

(RLDPE), through the thermally induced phase inversion method (TIPS). The membrane fabrication process involved the use of 8 wt% recycled LDPE in Butyl Acetate (BA) and the addition of 5% alumina powder.

The obtained membrane was characterized, and the results revealed several positive properties. The membrane exhibited good hydrophobicity, as indicated by a contact angle of 115°. This hydrophobic nature is beneficial for membrane distillation processes, as it promotes the selective permeation of vapor while repelling liquid water.

Furthermore, the membrane displayed a porosity of 65%, which indicates the presence of sufficient pores for efficient vapor transport. The mechanical properties of the membrane were also evaluated, with the strain at break measured at 117%, indicating its excellent elasticity and ability to withstand deformation without fracturing. Additionally, the membrane exhibited a significant and applicable elastic modulus value, highlighting its strength and structural integrity. To assess its performance, the obtained membrane was tested in vacuum membrane distillation. The results were promising, as the permeate flux achieved by the membrane was comparable to the values reported in the literature.

Abbreviations

RLDPE	Recycled low-density polyethylene
TIPS	Thermal induced phase separation
FTIR	Fourier transforms infrared spectroscopy
CA	Contact angle
mi	Total mass of water vapor
A	Effective membrane area
Θ	Young angle
θ^*	Wenzel contact angle
r	Roughness ratio
a	Actual microscopic area
MD	Membrane distillation
RO	Reverse osmosis
MED	Multiple Effect Distillation
MSF	Multi-stage flashing
PE	Polyethylene
PP	Polypropylene
SVMD	Solar vacuum membrane distillation
VMD	Vacuum membrane distillation

Acknowledgements

Not applicable.

Author contributions

HA is the main author, he had proposed the subject of this research, and he is responsible for the planning KH did the implementation of this research and was a major contributor to the writing of the manuscript, FK, HA, BC, AQ are responsible for discussing its results. All authors have read and approved the final version.

Funding

Not applicable.

Availability of data and materials

All data generated or analyzed during this study are included in this published article.

Declarations

Ethics approval and consent to participate

Not applicable.

Consent for publication

Not applicable.

Competing interests

The authors declare that they have no competing interests.

Received: 16 June 2023 Accepted: 12 August 2023

References

Abdallah H, Moustafa AF, Adnan Al H (2014) Performance of a newly developed titanium oxide nanotubes/polyethersulfone blend membrane for water desalination using vacuum membrane distillation. Desalination 346:30–36

Abedini R, Omidkhah M, Dorosti F (2014) CO_2/CH_4 separation by a mixed matrix membrane of polymethylpentyne/MIL-53 particles. Iran J Polym Sci Technol 27:337–351

Ajari H, Chaouachi B, Galiano F, Marino T, Russo F, Figoli A (2019) A novel approach for dissolving crystalline LDPE using non-toxic solvents for membranes preparation. J Environ Sci Telgy 16:5375–5386

Aljumaily MM, Alsaadi MA, Hashim NA, Alsalhy QF et al (2019) Embedded high-hydrophobic CNMs prepared by CVD technique with PVDF-co-HFP membrane for application in water desalination by DCMD Desalin. Water Treat 142:37–44

Alkhudhiri A, Naif D, Nidal H (2012) Membrane distillation: a comprehensive review. Desalination 287:2–18

Asma H, Khaoula H, Bechir C (2021). Manufacture of Hydrophobic Membranes Using Recycled Polymers for the Brackish Water Distillation. https://doi.org/10.1109/IREC48820.2020.9310400.11thIntRenEngyIREC2021

Asma H, Khaoula H, Bechir C (2022) Comparative study of the performance of a locally manufactured membrane and the commercial one in vacuum membrane distillation of brackish water Desa. Water Treat 247:10–16

Asma H, K Hidouri, B Chaouachi (2020) Manufacture of hydrophobic membranes using recycled polymers for the brackish water distillation. In: 11th International Renewable Energy Congress (IREC), Hammamet, Tunisia

Chang J, Zuo J, Lu K, Chung T-S (2019) Membrane development and energy analysisof freeze desalination- vacuum membrane distillation hybrid systems powered by LNG regasification and solar energy. Desalination 449:16–25

Cipollina A, Di Sparti MG, Tamburini A, Micale G (2012) Development of a membrane distillation module for solar energy seawater desalination. Chem Eng Resea and Design 90(12):2101–2121

El-Bourawi MS, Ding Z, M khayet, (2006) A framework for better understanding membrane distillation separation process. J Membr Sci 285(1–2):4–29

Fatma K, Béchir C, Hidouri K (2017) Study of vacuum membrane distillation coupled with solar energy. Int Conf Gre Engy Conv Syst (GECS). https://doi.org/10.1109/GECS.2017.8066220

Hamad K, Kaseem M, Deri F (2013) Recycling of waste from polymer materials: an overview of the recent works. Polym Degr Stab 98:2801–2812

Ji GL, Li-Ping Z, Bao-Ku Z, You-Yi X (2008) Structure formation and characterization of PVDF hollow fiber membrane prepared via TIPS with diluent mixture. J Mem Sci 319:264–270

Khaled F, Hidouri K, Criscuoli A et al (2020) Supply of solar energy in vacuum membrane distillation. J Am Eengy. https://doi.org/10.1080/01430750.2020.1789738

Kui W. A.A Ahmed, Mohammad A. Khaleel (2017) Mechanical properties of water desalination and waste water treatment membranes. Desal 190–205

Lloyd DR (1990) Microporous membrane formation via thermally induced phase separation. I. Solid-liquid phase separation. J Mem Sci 52:239–261

Ma B, Ding Y, Li W, Hu Ch, Yang M (2018) Ultrafiltration membrane fouling induced by humic acid with typical inorganic salts. Chemosphere 197:793–802

Malinalli RM, Sandra LA, Gyorgy S, Suzana PN (2023) Bio-Based Solvents for Polyolefin Dissolution and Membrane Fabrication: From Plastic Waste to Value-Added Materials. Gre Chemtry 25(3):966–977

Marino T, Galiano F, Molino A, Figoli A (2019) New frontiers in sustainable membrane preparation: Cyrene™ as green bioderived solvent. Jof Memb Sci 580:224–234

Mustafa MA, Haiyam MA, Ahmed AM et al (2022) The influence of coating super-hydrophobic carbon nanomaterials on the performance of membrane distillation. Appl Water Sci 12:28. https://doi.org/10.1007/s13201-021-01564-5

Rasool MA, Vankelecom IFJ (2021) Preparation of full-bio-based nanofiltration membranes. J Mem Sci 618:118674

Seyedpour SF, Rahimpour A, Mohsenian H, Taherzadeh MJ (2018) Low fouling ultrathin nanocomposite membranes for efficient removal of manganese. J Membr Sci 549:205–216

Tobo-Niño OM, García-Jiménez CD, Muvdi-Nova CJ (2017) Flat sheet membrane elaboration by TIPS method using palm oil as solvent and its application in membrane distillation. Ingeniería y Competitividad 19:81–90

Vinci RP, VlassakJ.J, (1996) Mechanical behavior of thin films, Annuel Revue Materiel. Science 26:431–462

Wang P, Chung TS (2015) Recent advances in membrane distillation processes: Membrane development, configuration design and application exploring. J Member Sci 474:39–56

Wenzel RN (1936) Resistance of solid surfaces to wetting by water. Ind Eng Chem 28:988–994

Yongqing W, Zhilong Xu, Noam L (2015) An experimental study of solar thermal vacuum membrane distillationdesalination. Desal and Wat Trea 53:887–897

Publisher's Note